

Femtosecond relativistic electron beam with reduced timing jitter from THz-driven beam compression

Lingrong Zhao^{1,2}, Heng Tang^{1,2}, Chao Lu^{1,2}, Tao Jiang^{1,2}, Pengfei Zhu^{1,2}, Long Hu³, Wei Song³, Huida Wang³, Jiaqi Qiu⁴, Chunguang Jing⁵, Sergey Antipov⁵, Dao Xiang^{1,2,6*} and Jie Zhang^{1,2*}

¹ Key Laboratory for Laser Plasmas (Ministry of Education),

School of Physics and Astronomy,

Shanghai Jiao Tong University, Shanghai 200240, China

² Collaborative Innovation Center of IFSA (CICIFSA),

Shanghai Jiao Tong University, Shanghai 200240, China

³ Science and Technology on High Power Microwave Laboratory,
Northwest Institute of Nuclear Technology,

Xi'an, Shanxi 710024, China

⁴ Nuctech Company Limited, Beijing, 100084, China

⁵ Euclid Techlabs LLC, Bolingbrook, Illinois 60440, USA

⁶ Tsung-Dao Lee Institute, Shanghai 200240, China

(Dated: January 19, 2022)

We propose and demonstrate a novel method to reduce the pulse width and timing jitter of a relativistic electron beam through THz-driven beam compression. In this method the longitudinal phase space of a relativistic electron beam is manipulated by a linearly polarized THz pulse in a dielectric tube such that the bunch tail has a higher velocity than the bunch head, which allows simultaneous reduction of both pulse width and timing jitter after passing through a drift. In this experiment, the beam is compressed by more than a factor of four from 130 fs to 28 fs with the arrival time jitter also reduced from 97 fs to 36 fs, opening up new opportunities in using pulsed electron beams for studies of ultrafast dynamics. This technique extends the well known rf buncher to the THz frequency and may have a strong impact in accelerator and ultrafast science facilities that require femtosecond electron beams with tight synchronization to external lasers.

PACS numbers:

Ultrashort electron beams with small timing jitter with respect to external lasers are of fundamental interest in accelerator and ultrafast science communities. For instance, such beams are essential for laser and THz-driven accelerators ([1–4]) where the beam energy spread and beam energy stability largely depend on the electron bunch length and injection timing jitter, respectively. For MeV ultrafast electron diffraction (UED [5–12]) where ultrashort electron beams with a few MeV energy are used to probe the atomic structure changes following the excitation of a pump laser, the temporal resolution is primarily limited by the electron bunch length and timing jitter. Similar limitations exist for x-ray free-electron lasers (FEL [13–15]) too, since the properties of the x-ray pulses depend primarily on that of the electron beams. Therefore, one of the long-standing goals in accelerator and ultrafast science communities is to generate ultrashort electron beams with small timing jitter.

Photocathode rf gun is the leading option for producing high brightness ultrashort electron beam for FEL and MeV UED (see, e.g. [16, 17]). Due to space charge effect, the electron beam pulse width is broadened and therefore bunch compression is typically needed to reduce the pulse width. Bunch compression requires first a mechanism to imprint energy chirp (correlation between an electron's energy and its longitudinal position) and then sending the beam through a dispersive element such that the longitudinal displacement of the electrons is changed

in a controlled way for reducing the pulse width. For MeV beam, this is typically achieved by first sending the beam through a rf buncher cavity at zero-crossing phase where the bunch head ($t < 0$) is decelerated while the bunch tail ($t > 0$) is accelerated. This imprints a negative chirp $h = d\delta/cdt < 0$ in the beam longitudinal phase space, where δ is the relative energy difference of an electron with respect to the reference electron and c is the speed of light. Then the electron beam is sent through a drift after which the electrons at the bunch tail catch up with those at the bunch head, leading to compression in pulse width. Full compression is achieved when $hR_{56} = -1$, where $R_{56} \approx L/\gamma^2$ is the momentum compaction of the drift with length L and γ is the Lorentz factor of the electron beam.

Recently, sub-10 (rms) fs beams have been produced with this rf buncher technique [18, 19]. However, the rf phase jitter results in increased beam timing jitter after compression. While THz pulse based time-stamping techniques have been developed to measure and correct the electron beam arrival time jitter [19, 20] for UED, the detector response time limited this shot-to-shot correction technique to low repetition rate. It is highly desired (in particular for those experiments that require long data acquisition time (see, e.g. [21])) if the beam can be compressed without increasing the jitter such that time-stamping technique is not needed. Many efforts have been devoted towards this goal in the past few

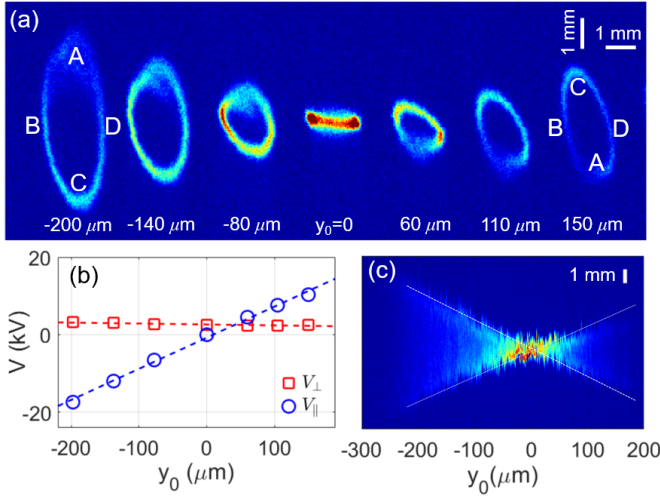


FIG. 2: Beam distributions at screen P2 (a) and longitudinal and transverse energy kicks (b) for various offsets in D1. Note, for the purpose of illustration, the horizontal axis in (a) represents time and vertical axis represents energy. The superimposed beam distribution on P2 for a fine scan of offsets in D1 is shown in (c).

linearly with transverse offset.

The maximal energy change of the electrons can be found using the distance between A and C in Fig. 2a. Similarly, the maximal transverse energy kick can be found using the distance between B and D. After converting the distance into voltage using the known dispersion, the longitudinal energy kick from longitudinal electric field (V_{\parallel}) and transverse energy kick (V_{\perp}) from transverse electromagnetic field are shown in Fig. 2b. The transverse kick is independent of the transverse offset and the longitudinal kick scales linearly with the offset. In a separate experiment, the beam distribution at P2 is measured with a fine scan of y_0 and the distributions are then superimposed and shown in Fig. 2c where a cone shape (guided with the dotted line) is clearly seen that shows the linear dependence of energy change on transverse offset.

A closer look at the rings in Fig. 2a indicates that the transverse kick and longitudinal kick have $\pi/2$ phase difference. For instance, electrons in regions A and C experience on-crest phase for acceleration but zero-crossing phase for deflection. To confirm this, the pulse stacker is removed and now a beam with about 130 fs pulse width is produced. The timing of the THz beam is varied and the beam centroid change as well as energy change are measured simultaneously and the results are shown in Fig. 3 which confirms the $\pi/2$ phase difference in acceleration and deflection. This $\pi/2$ phase difference results in a net shift of the beam centroid divergence during compression and thus can be straightforwardly corrected with a steering magnet. With the group velocity of the THz pulse being about $v_g \approx 0.84c$ in D1, the interaction window within which the electrons can catch up and interact with

the THz pulse in D1 is about $(c/v_g - 1)L_D/c \approx 10$ ps. This is the main reason that multiple oscillations are observed in Fig. 3 even when a single-cycle THz pulse is used.

To measure the time information of the compressed bunch, a second THz pulse is used to deflect the beam for converting time information into spatial distribution. In our first attempt, the second THz pulse is also vertically polarized as the crystals and gratings have the same configurations for the two THz sources. However, it is noted that such a configuration may introduce ambiguity in data interpretation. For instance, when the electron beam passes through both tubes on-axis, but with π difference in phase, then the deflection from the first THz pulse is canceled by the second THz pulse. This produces a transverse beam size comparable to that with full compression while apparently no compression occurs here. To allow unambiguous determination of the bunch compression effect, in our experiment a polarization rotation (PR) element consisting of a pair of wire grid polarizers and roof mirrors are used to manipulate the THz polarization. As shown in [26], by changing the path length of the two roof mirrors, a vertically polarized THz pulse can be converted into a horizontally polarized pulse.

Then we sent the electron beam through D1 at an offset of 200 μm , and used a steering magnet to center the beam in the second tube (D2). The beam distributions on screen P1 measured with the two THz pulses on for various time delay between the electron beam and first THz pulse are shown in Fig. 4. In this measurement the timing of the second THz pulse is adjusted such that the beam always rides at the zero-crossing phase of the deflection field. Fig. 4a-d corresponds to the cases when the electron beam is at regions A, B, C, and D in Fig. 2a, respectively. As shown in Fig. 4a and Fig. 4c, the beam is at on-crest phases for acceleration and at the zero-crossing phases for deflection in D1, so the beam is deflected vertically by the first THz pulse and deflected horizontally by the second THz pulse, leading to correlation in horizontal and vertical distribution. The beam is not compressed at these time delays. It should be noted that

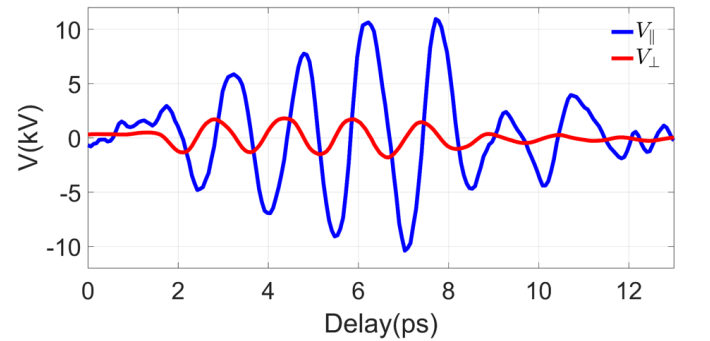


FIG. 3: Longitudinal and transverse energy kicks as a function of time delay between the first THz pulse and electron beam.

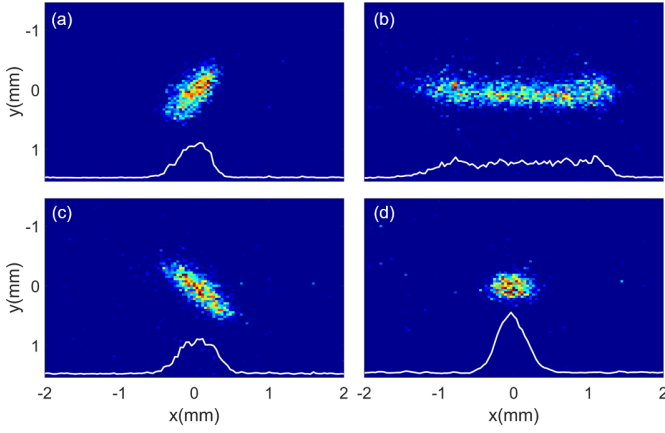


FIG. 4: Beam distributions at screen P1 measured with both THz pulses on for various time delays between the first THz pulse and the electron beam.

the streaked beam size is larger than the aperture of D2, so only part of the beam is measured on screen P1. The beam is at one of the zero-crossing phases for acceleration in Fig. 4b. However, at such phase the bunch head is accelerated while the bunch tail is decelerated. As a result, a positive energy chirp is imprinted in the beam phase space, leading to bunch lengthening by roughly a factor of 2. The bunch duration in this case is larger than the dynamic range of the measurement (roughly one quarter of the deflection wavelength), and thus a quasi-flat-top distribution is seen for the deflected beam.

Fig. 4d shows the distribution when the beam is at the right zero-crossing phase for bunch compression. For this case the beam is shorter than the dynamic range of the measurement and thus the bunch length can be accurately determined. In this measurement the ramping rate of the deflection from the second THz pulse is found to be about $4 \mu\text{m}/\text{fs}$. With the transverse beam size and beam centroid fluctuation at screen P1 measured to be about $120 \mu\text{m}$ and $16 \mu\text{m}$ with the THz off, the resolution of beam temporal profile measurement and the accuracy of beam arrival time measurement are determined to be about 30 fs and 4 fs, respectively. With the strength of the first THz pulse varied to provide the optimal energy chirp, full compression is achieved and the raw beam pulse width in Fig. 4d after converting the beam size to time is measured to be about 41 fs (rms). Subtracting the resolution in quadrature yields a true bunch length of about 28 fs (rms).

Under full compression condition, 50 consecutive measurements of the raw beam profile at P1 (with horizontal axis converted into time) with THz buncher off and on are shown in Fig. 5a and Fig. 5d, respectively. The effect of longitudinal compression can be clearly seen. The average bunch length (calculated by subtracting the contribution from intrinsic beam size) before and after THz compression is about 130 fs and 28 fs, respectively. The fluctuation of the beam centroid (black dots in Fig. 5a

and Fig. 5d) which represents the time jitter with respect to the second THz pulse is also greatly reduced from about 97 fs to about 36 fs after compression.

It should be noted that while the initial jitter before the THz buncher is greatly compressed, the energy stability of the beam still limits the residual timing jitter of the THz buncher scheme to $\Delta t = R_{56}\delta E/E$, where $\delta E/E$ is the relative energy stability of the beam. In this experiment, the beam energy stability is measured to be about 2.5×10^{-4} , which together with 3.9 cm momentum compaction from D1 to D2 leads to a residual timing jitter of about 32 fs, in good agreement with the experimental result. For keV UED with high energy stability, such timing jitter is negligible. With full compression, the residual bunch length is limited by the uncorrelated beam energy spread (σ_δ) to $\sigma_\delta R_{56}/E$. In our experiment, the beam uncorrelated energy spread grows in the THz buncher because of the linear dependence of the longitudinal electric field and the finite transverse beam size (about $20 \mu\text{m}$) in D1. The uncorrelated energy spread growth is estimated to be about 0.55 keV which results in a residual bunch length of about 24 fs, consistent with the measured value. The minimal bunch length may be further reduced by focusing the beam to a smaller size. It is also possible to use an additional dielectric tube to cancel the energy spread growth. For instance, after the THz buncher, the beam may be sent through a second tube on-axis. By using a THz pulse with π phase difference, the energy spread growth may be effectively canceled with the chirp unchanged. The residual timing jitter may be reduced with improved energy stability, or using a THz pulse with stronger strength [28] for lowering the required momentum compaction. Such steps should be able to push both the electron bunch length

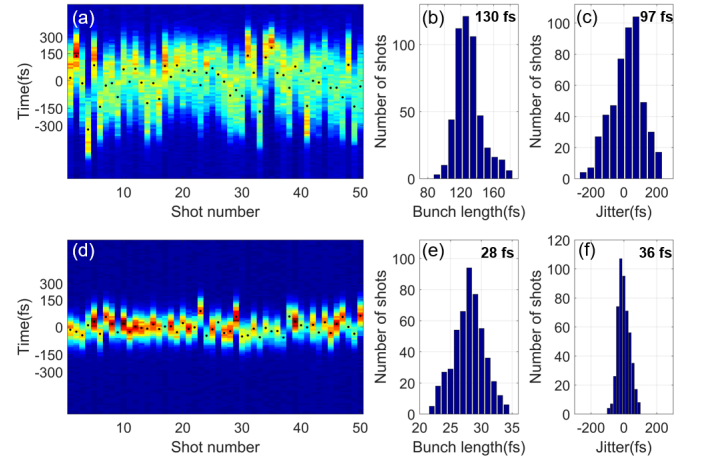


FIG. 5: 50 consecutive single-shot measurements of the beam temporal profile without (a) and with (d) the THz buncher, and the rms pulse width statistics collected over 500 consecutive shots without (b) and with (e) the THz buncher. The beam centroid for each individual shot (black dots) is used to determine the time jitter without (c) and with (f) the THz buncher.

and arrival time jitter to sub-10 fs regime, opening up new opportunities in ultrafast science and advanced acceleration applications.

In conclusion, we have demonstrated a novel method to manipulate relativistic beam phase space for longitudinal compression. By using the longitudinal field in HEM11 mode for imprinting the energy chirp and with the THz pulse co-propagating with the electron beam, the mode is easily excited with a linearly polarized THz pulse and the required THz pulse energy for producing sufficient energy chirp is greatly reduced. In our experiment we have demonstrated significant reduction in both bunch length and arrival time jitter, which may allow one to significantly enhance the temporal resolution of UED. The demonstrated colinear interaction scheme is also of inter-

est for THz-driven beam acceleration that holds potential for downsizing accelerator-based large scientific facilities such as FELs and colliders. We expect this THz-driven beam manipulation method to have wide applications in many areas of researches.

This work was supported by the Major State Basic Research Development Program of China (Grants No. 2015CB859700) and by the National Natural Science Foundation of China (Grants No. 11327902, 11504232 and 11721091). One of the authors (DX) would like to thank the support of grant from the office of Science and Technology, Shanghai Municipal Government (No. 16DZ2260200 and 18JC1410700).

* dxiang@sjtu.edu.cn

* jzhang1@sjtu.edu.cn

-
- [1] R. England *et al.*, *Dielectric laser accelerators*, Rev. Mod. Phys. 86, 1337 (2014).
 - [2] E. A. Nanni, W. R. Huang, K. Ravi, A. Fallahi, G. Moriena, R. J. Miller, and F. X. Kartner, *Terahertz-driven linear electron acceleration*, Nat. Commun. 6, 8486 (2015).
 - [3] D. Zhang *et al.*, *Segmented terahertz electron accelerator and manipulator (STEAM)*, Nat. Photonics 12, 336 (2017).
 - [4] E. Curry, S. Fabbri, J. Maxson, P. Musumeci, and A. Gover, *Meter-Scale Terahertz-Driven Acceleration of a Relativistic Beam*, Phys. Rev. Lett. 120, 094801 (2018).
 - [5] J. Hastings, F. Rudakov, D. Dowell, J. Schmerge, J. Cardoza, J. Castro, S. Gierman, H. Loos, and P. Weber, *Ultrafast time-resolved electron diffraction with megavolt electron beams*, Appl. Phys. Lett. 89, 184109 (2006).
 - [6] P. Musumeci, J. Moody, C. Soby, M. Gutierrez, H. Bender, and N. Wilcox, *High quality single shot diffraction patterns using ultrashort megaelectron volt electron beams from a radio frequency photoinjector*, Rev. Sci. Instrum. 81, 013306 (2010).
 - [7] R. Li *et al.*, *Experimental demonstration of high quality MeV ultrafast electron diffraction*, Rev. Sci. Instrum. 81, 036110 (2010).
 - [8] Y. Murooka, N. Naruse, S. Sakakihara, M. Ishimaru, J. Yang, and K. Tanimura, *Transmission-electron diffraction by MeV electron pulses*, Appl. Phys. Lett. 98, 251903 (2011).
 - [9] F. Fu, S. Liu, P. Zhu, D. Xiang, J. Zhang, and J. Cao, *High quality single shot ultrafast MeV electron diffraction from a photocathode radio-frequency gun*, Rev. Sci. Instrum. 85, 083701 (2014).
 - [10] P. Zhu *et al.*, *Femtosecond time-resolved MeV electron diffraction*, New J. Phys. 17, 063004 (2015).
 - [11] S. Weathersby *et al.*, *Mega-electron-volt ultrafast electron diffraction at SLAC National Accelerator Laboratory*, Rev. Sci. Instrum. 86, 073702 (2015).
 - [12] S. Manz *et al.*, *Mapping atomic motions with ultrabright electrons: towards fundamental limits in space-time resolution*, Faraday Discuss. 177, 467 (2015).
 - [13] P. Emma *et al.*, *First lasing and operation of an angstrom-wavelength free-electron laser*, Nat. Photonics 4, 641 (2010).
 - [14] T. Ishikawa *et al.*, *A compact X-ray free-electron laser emitting in the sub-angstrom region*, Nat. Photonics 6, 540 (2012).
 - [15] H. Kang *et al.*, *Hard X-ray free-electron laser with femtosecond-scale timing jitter*, Nat. Photonics 11, 708 (2017).
 - [16] X. Wang, D. Xiang, T. Kim, and H. Ihee, *Potential of Femtosecond Electron Diffraction Using Near-Relativistic Electrons from a Photocathode RF Electron Gun*, J. Korean Phys. Soc. 48, 390 (2006).
 - [17] R. Akre *et al.*, *Commissioning the Linac Coherent Light Source injector*, Phys. Rev. ST Accel. Beams 11, 030703 (2008).
 - [18] J. Maxson, D. Cesar, G. Calmasini, A. Ody, P. Musumeci, and D. Alesini, *Direct measurement of sub-10 fs relativistic electron beams with ultralow emittance*, Phys. Rev. Lett. 118, 154802 (2017).
 - [19] L. Zhao *et al.*, *Terahertz Streaking of Few-Femtosecond Relativistic Electron Beams*, Phys. Rev. X, 8, 021061 (2018).
 - [20] R.K. Li *et al.*, *Terahertz-based attosecond metrology of relativistic electron beams*, Phys. Rev. Accel. Beams 22, 012803 (2019).
 - [21] J. Yang *et al.*, *Imaging CF3I conical intersection and photodissociation dynamics with ultrafast electron diffraction*, Science 361, 64 (2018).
 - [22] C. Kealhofer, W. Schneider, D. Ehberger, A. Ryabov, F. Krausz, and P. Baum, *All-optical control and metrology of electron pulses*, Science 352, 429 (2016).
 - [23] D. Ehberger, K. Mohler, T. Vasileiadis, R. Ernstorfer, L. Waldecker, and P. Baum, *Terahertz Compression of Electron Pulses at a Planar Mirror Membrane*, Phys. Rev. Applied 11, 024034 (2019).
 - [24] J. Hebling, G. Almási, I. Kozma, and J. Kuhl, *Velocity matching by pulse front tilting for large area THz-pulse generation*, Opt. Express 10, 1161 (2002).
 - [25] T. Grosjean *et al.*, *Linear to radial polarization conversion in the THz domain using a passive system*, Opt. Express 16, 18895 (2008).
 - [26] L. Zhao *et al.*, *Terahertz Oscilloscope for Recording Time Information of Ultrashort Electron Beams*, Phys. Rev. Lett. 122, 144801 (2019).
 - [27] W. Panofsky and W. Wenzel, *Some Considerations Con-*

- cerning the Transverse Deflection of Charged Particles in RadioFrequency Fields*, Rev. Sci. Instrum. 27, 967 (1956).
- [28] H. Hirori, A. Doi, F. Blanchard, and K. Tanaka, *Single-cycle terahertz pulses with amplitudes exceeding 1 MV/cm generated optical rectification in LiNbO₃*, Appl. Phys. Lett. 99, 091106 (2011).